Journal of Colloid and Interface Science 645 (2023) 715–723

Contents lists available at ScienceDirect

Journal of Colloid And Interface Science

journal homepage: www.elsevier.com/locate/jcis

Uranium surface processes with sandstone and volcanic rocks in acidic and alkaline solutions

Janice P.L. Kenney [a,b,*], Juan Lezama-Pacheco [c], Scott Fendorf [c], Daniel S. Alessi [d], Dominik J. Weiss [a,c,*]

[a] Earth Science and Engineering, Imperial College London, London, United Kingdom
[b] Department of Physical Sciences, MacEwan University, Edmonton, Alberta, Canada
[c] Earth Systems Science Department, Stanford University, Stanford, United States of America
[d] Department of Earth and Atmospheric Sciences, University of Alberta, Edmonton, Canada

GRAPHICAL ABSTRACT

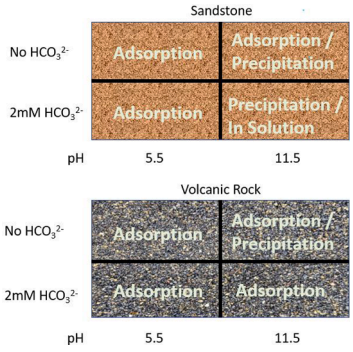

ARTICLE INFO

Keywords:
Adsorption
Precipitation
Uranium
EXAFS
FTIR
Surface complexation modelling
Radioactive waste disposal

ABSTRACT

Understanding the behaviour of uranium waste, for disposal purposes, is crucial due to the correlation between pH values and the disposal of distinct types of waste, with low level waste typically associated with acidic pH values, and higher and intermediate level waste commonly related to alkaline pH values. We studied the adsorption of U(VI) on sandstone and volcanic rock surfaces at pH 5.5 and 11.5 in aqueous solutions with and without bicarbonate (2 mM HCO_3^-) using XAS and FTIR. In the sandstone system, U(VI) adsorbs as a bidentate complex to Si at pH 5.5 without bicarbonate and as uranyl carbonate species with bicarbonate. At pH 11.5 without bicarbonate, U(VI) adsorbs as monodentate complexes to Si and precipitates as uranophane. With bicarbonate at pH 11.5, U(VI) precipitated as a Na-clarkeite mineral or remained as a uranyl carbonate surface species. In the volcanic rock system, U(VI) adsorbed to Si as an outer sphere complex at pH 5.5, regardless of the presence of bicarbonate. At pH 11.5 without bicarbonate, U (VI) adsorbed as a monodentate complex to one Si atom and precipitated as a Na-clarkeite mineral. With bicarbonate at pH 11.5, U(VI) sorbed as a bidentate carbonate complex to one Si atom. These results provide insight into the behaviour of U(VI) in heterogeneous, real-world systems related to the disposal of radioactive waste.

* Corresponding authors at: Department of Physical Sciences, MacEwan University, Edmonton, Alberta, Canada (Janice P.L. Kenney).
E-mail addresses: janice.kenney@macewan.ca (J.P.L. Kenney), d.weiss@imperial.ac.uk (D.J. Weiss).

https://doi.org/10.1016/j.jcis.2023.04.174
Received 30 January 2023; Received in revised form 26 April 2023; Accepted 30 April 2023
Available online 6 May 2023

1. Introduction

Radioactive wastes are stored at or near the surface, with long term plans of eventual deep geologic storage for some of the wastes (intermediate-level waste (ILW) and high heat generating wastes) [50]. Underground storage of wastes will be coupled with further cement backfill, which will lead to high pH values (pH 10–13.5) in the near field of the wastes for thousands of years [30]. Radioactive low-level waste (LLW) and ILW will be disposed of in drums filled with cement, which will solidify and fill voids within the waste while reducing radiation exiting the drum. In deep geologic storage where reducing conditions exist, uranium (U) is likely to be present as U(IV) species, which may subsequently precipitate to form uraninite [13]. However, there remains uncertainty around potential re-oxidation of U(IV) to U(VI) if the system is exposed to a future influx of oxidising groundwaters or from oxidants produced by the irradiation of water by radioactive waste [19]. Therefore, consideration of U(VI) species remains important in developing an environmental safety case in the deep geologic disposal of radioactive waste, as they tend to be more mobile than U(IV) species.

LLW will be disposed of in high pH generating vaults, as well as in trenches - some with no cement [30]. The degradation of cellulosic materials and corrosion of metals would lead to lower pH environments (pH 3–6) in those systems [17]. The disposal of LLW will likely be in the vadose zone, where U is likely to be present as a U(VI) species. Depending on the disposal regime, U may be present as a range of uranyl (hydr)oxide and carbonate species over a pH range of 3–13.5, with U minerals expected to form at high pH [37,8,4,47,40,40]. Therefore, if U becomes mobilised in one of the above disposal scenarios, it is important to understand how it may interact with the surrounding rocks to aid in predicting potential contamination of aquifers or surface waters.

Many studies have investigated the removal of U from solution via single mineral systems [60,22,46,6,56,60,15] and less with complex heterogeneous real rocks and sediments or complex mixtures of minerals [22,59,51,5,39]. Two significant modes of uranium (U) removal from solution have been generally observed in the presence of a range of rocks and minerals, as the pH is varied from 2 to 12. Kenney et al. [39] reported there to be a sorption envelope in the range of pH 4–8 and an envelope controlled by U(VI) precipitation between pH 10–12, and saw little removal between pH 8–10 for sandstone and crystalline volcanic rock. This dip between pH 8–10 was believed to be due to the persistence of the negatively charged uranyl species which interact with predominantly negatively charged surfaces (e.g., [59,46,51,23,31,11,39]). For example, when high concentrations of carbonates are found in, or are added to, the U-containing solution, U forms negatively charged species that include $UO_2(CO_3)_3^{4-}$ in alkaline solutions which does not readily sorb to rocks or minerals [37,29,40,40].

Ensuring the safe and effective disposal of radioactive waste is a matter of utmost importance, but the way to achieve it is often a subject of controversy [7]. There have been numerous debates in various countries regarding the optimal geological and geographical locations for storing such hazardous materials. It is increasingly crucial to understand how the geology of a disposal site may interact with any potential release of radionuclides. In our previous work [39], we investigated the crystalline basement rock (Borrowdale Volcanic Group) and a potential aquifer rock (St. Bees Sandstone), which have been extensively studied and discussed in the context of the United Kingdom, in terms of their suitability to act as areas that may be at risk of contamination in the event of waste leakage from a future Geological Disposal Facility or near-surface storage of waste [30]. Specifically, we [39] studied the removal of U from solution as a function of pH, U concentration, and bicarbonate content onto the sandstone and volcanic rock. We found that when bicarbonate was added to the system, U was removed from solution in a bimodal manner, as explained above. When bicarbonate was not added to the system, U was assumed to be removed solely through adsorption over a broader pH range of 4 to 12 via the rock surface or precipitation of a sodium uranate mineral suspended in solution, based on aqueous speciation modelling. While we [39] were able to determine the extent of U removal from solution by the two rocks with and without the addition of bicarbonate, the molecular bonding environment of U was not determined.

The objective of our current research is to advance the understanding of molecular-level interactions by which sandstone and volcanic rock are capable of removing U from solution, building upon our previous study [39]. Specifically, our goal is to investigate the adsorption (at pH 4–8) and precipitation (at pH 10–12) regimes identified in the previous study, aiming to provide a comprehensive understanding of the intricate processes, whether adsorption or precipitation reactions, involved in U removal from solution by these geological materials. To do this, the rocks were first characterised by modelling potentiometric titration data to develop surface complexation models to quantify the proton-active surface sites available for U binding. Batch experiments were subsequently conducted and the rocks with were analysed using extended X-ray absorption fine structure (EXAFS) spectroscopy to understand how the U is bound to functional groups on the rocks and/or if there is U precipitation. Experiments were conducted at pH 5.5 and 11.5, to test the assumptions in Kenney et al. [39], that at pH 5.5 U was adsorbed to the surface of the rocks and at pH 11.5 U was precipitated as a sodium uranate mineral. Fourier transform infrared (FTIR) spectroscopy was used to confirm that there was no change in the mineralogy of the rocks over the course of the experiments.

2. Materials and methods

2.1. Solution and rock preparation

St. Bees Sandstone, which is an iron-coated sandstone, and volcanic rock from the Borrowdale Volcanic group were collected from Cumbria, UK, as they were rocks from a site that was previously considered for disposal of wastes in the UK [30]. The rocks were crushed and sieved to between 128 and 700 mm before being washed, using the same procedure as Kenney et al. [39], to remove surface contaminants. Briefly, this washing procedure employed a 1 M NaOH wash, lasting less than 2 min, followed by a rinse with 18.2 MΩ water, repeated two times. This procedure was used to ensure the same methods were followed as in Kenney et al. [39] and because it has been shown to be an effective way to remove surface impurities to ensure the rock particles are cleaned prior to experiments [66,42,32]. Following the washing, the sandstone and volcanic rocks were dried at 45 °C for 24 h. The rocks used in this study are the same as those used in Kenney et al. [39], with a specific surface area (BET) of 1.3496 m^2/g for the sandstone and 0.7549 m^2/g for the volcanic rock. Kenney et al. [39] determined from X-ray diffraction (XRD) analyses that the sandstone was comprised of mostly quartz with some microcline and mica, with an iron coating, which was assumed to be hematite. The volcanic rock consisted of quartz, chlorite, mica, plagioclase, and calcite.

Uranium solutions of 10 ppm were prepared using a 1000 ppm standard U(VI) nitrate stock solution (VWR). This concentration of U was chosen to better compare our results to the study by Kenney et al. [39]. All solutions were diluted with 0.1 M NaCl, to buffer the ionic strength and mimic a mild groundwater salinity, to reach the desired U concentrations in this study. Sodium bicarbonate stock solutions (Sigma Aldrich) of 0.1 M were prepared and used to spike bicarbonate-containing solutions and suspensions to a $NaHCO_3$ concentration of 2 mM.

2.2. Potentiometric titrations

Potentiometric titrations were conducted on suspensions of sandstone and volcanic rock (15–90 g/L) using a method similar to Kenney et al. [38]. The suspensions were buffered for ionic strength using 0.1 M NaCl, which was bubbled with N_2 for 30 min prior to titration. Titrations were conducted under an N_2 atmosphere and were continuously stirred

with a magnetic stir bar to ensure the crushed rock remained suspended. Each titration was carried out a minimum of two times in each direction (2x forward and reverse titrations) on the sandstone and the volcanic rock suspensions, using a Metrohm 888 Titrando automated burette assembly and pH measurements were conducted with a ROSS SLS semi micro glass combination electrode filled with 0.1 M NaCl. The rock suspensions were first acidified to pH 2.5 using 1.0 M HCl and aliquots of 1.0 M NaOH were added to raise the pH of the suspensions to approximately pH 10.5 (forward titration) before being lowered again to pH 2.5 (reverse titration) using 1.0 M HCl, to test the reversibility of proton binding and to ensure that the minerals did not undergo significant dissolution during the titrations.

2.3. Surface complexation modelling

Titration data from the sandstone and volcanic rock were modelled using a discrete proton-active site surface complexation model, following the approach developed by Fein et al. [26]. The functional groups on the rocks are represented by distinct sites that deprotonate according to the following reaction:

$$R - Site_X H^\circ \leftrightarrow R - Site_X^- + H^+ \quad (1)$$

where R represents the rock surface to which each type of functional group, $Site_X$, is attached. The equilibrium constant (K_a) for this reaction is expressed as:

$$K_a = [R - Site_X^-]^* \alpha_{H+} / [R - Site_X H^\circ] \quad (2)$$

where R is the bulk rock, [R–$Site_X^-$] and [R–$Site_X H^\circ$] represent the concentrations of the deprotonated and protonated form of site type $Site_X$, respectively, and α_{H+} represents the activity of protons in solution. Experimental data for proton sorption to the rocks were modelled with a non-electrostatic surface complexation model using the computer programme FITEQL 2.0 [64]. The non-electrostatic model (NEM) approach has been applied to describe the surface sites of multi-components systems such as mineral assemblages [18,49,1], bacterial cells [10,35,38], and organic-mineral composites [2]. The resulting models allow for prediction of the sorption of actinides to the surfaces of these rocks under dynamic environmental conditions.

2.4. EXAFS and FTIR sample preparation

Batch experiments were conducted in a in the same manner to those described in Kenney et al. [39]. Briefly, we used suspensions of crushed sandstone or volcanic rock (~5 g/L), with initial U(VI) solution concentrations of 10 ppm in 0.1 M NaCl electrolyte solution, with and without the addition of 2 mM $NaHCO_3$. The uranyl solutions were made by diluting the 1000 ppm U(VI) stock solution with 0.1 M NaCl, after which the pH of the solutions was adjusted to 5.2–5.7 or 11.3–11.6 (referred to as 5.5 of 11.5 throughout), and those ranges chosen from areas of increased removal from solution noted by Kenney et al. [39]. The total mass of rock for each sample was 1.0 g. Following the protocol outlined in Kenney et al. [39], each sample was left to react for a period of three days. Samples were divided into subsets, part of which was used for EXAFS measurements and part for FTIR analysis. Aliquots were also taken to measure total U concentration by inductively coupled plasma mass spectroscopy (ICP-MS) analysis, to later calculate U removal from solution by the rocks. The details of the experimental conditions for each of the samples are outlined in Table 1.

2.5. FTIR spectroscopic data collection and analysis

FTIR spectroscopy was used to ensure that mineralogical changes to the rocks (e.g. dissolution or precipitation of secondary minerals) did not occur during the experiments and, insofar as possible, to detect the adsorption or precipitation of U at the mineral surface. Samples were analysed on a Nicolet 5700 Spectrometer using a diamond ATR crystal. A background spectrum, with 128 scans and a spectral resolution of 4 cm^{-1}, was taken of the empty ATR crystal before spectra were recorded of the subset of dried samples. The dried samples were pressed onto the ATR crystal and 128 scans with a spectral resolution of 4 cm^{-1} were recorded for each sample. The spectra were baseline corrected using asymmetric least squares fitting [25] with parameters $\lambda = 20{,}000$ and $p = 0.001$, smoothed using a Savitzky–Golay filter [55] and area-normalized from 1200 to 800 cm^{-1} using a previously developed script [27].

Table 1
Sample conditions for the U-removal batch experiments.

Sample name	Rock type	U(VI) (M)	HCO_3^- (mM)	pH after reaction	Amount of rock in suspension (g/L)
SS 5	Sandstone	4.20E-05	0	5.2	4.23
SS 5 HCO_3^-	Sandstone	4.20E-05	2	5.2	4.57
SS 11.5	Sandstone	4.20E-05	0	11.3	5.61
SS 11.5 HCO_3^-	Sandstone	4.20E-05	2	11.3	4.66
BVG 5.5	Volcanic rock	4.20E-05	0	5.5	4.94
BVG 5.5 HCO_3^-	Volcanic rock	4.20E-05	2	5.7	4.58
BVG 11.5	Volcanic rock	4.20E-05	0	11.6	5.09
BVG 11.5 HCO_3^-	Volcanic rock	4.20E-05	2	11.4	4.78

2.6. EXAFS spectra collection and data analysis

EXAFS spectra were collected at the U L_{III}-edge (17.116 keV) at Beamline 4–1 of the Stanford Synchrotron Radiation Lightsource (SSRL), USA. Approximately 10 mg of each dry sample was loaded without dilution into Al X-ray cells (1 mm thick) with Kapton windows. Samples were mounted at the cold finger of a liquid N2 cryostat. U LIII-fluorescence spectra were collected using a typical beam size of 5–10 mm, using detuned Si (2 2 0) double-crystal monochromators calibrated with an Y foil (K-edge at 17038.4 eV).

The EXAFS spectra were processed using SIXPACK and the Horae program suite [63]. Backscattering phase and amplitude functions required for fitting of spectra were obtained from FEFF8. Data were fit using Artemis, using the Fourier transformed signal of the EXAFS spectra (R-space).

3. Results

3.1. Characterisation of sandstone and volcanic rock

3.1.1. Fourier transform infrared spectroscopy

FTIR spectroscopy was used to monitor changes in the sandstone and volcanic rock before and after reacting for three days with the 10 ppm U (VI) solution, at pH 5.5 and 11.5, with and without the presence of HCO_3^-. The FTIR spectra for sandstone, volcanic rock, as well as quartz, chlorite, and goethite reference materials, are given in Fig. 1. Kenney et al. [39] found that the sandstone is predominantly made up of quartz, using XRD analysis. FTIR spectroscopy in this study noted the presence of quartz with dominant peaks at 1195, 1161, and 1078 cm^{-1}, which match those peaks for the Si-O bonds in the quartz standard. Further peaks were identified in the sandstone at 1054 and 1006 cm^{-1}, which were assumed to be those of microcline [58]. The goethite standard had a peak at 890 cm^{-1}, which represents the Fe—O—H band, and which is lower than the peak we observed at 912 cm^{-1} for the sandstone. The Fe—O—H band appearing at 916 cm^{-1} is consistent with hematite [53]

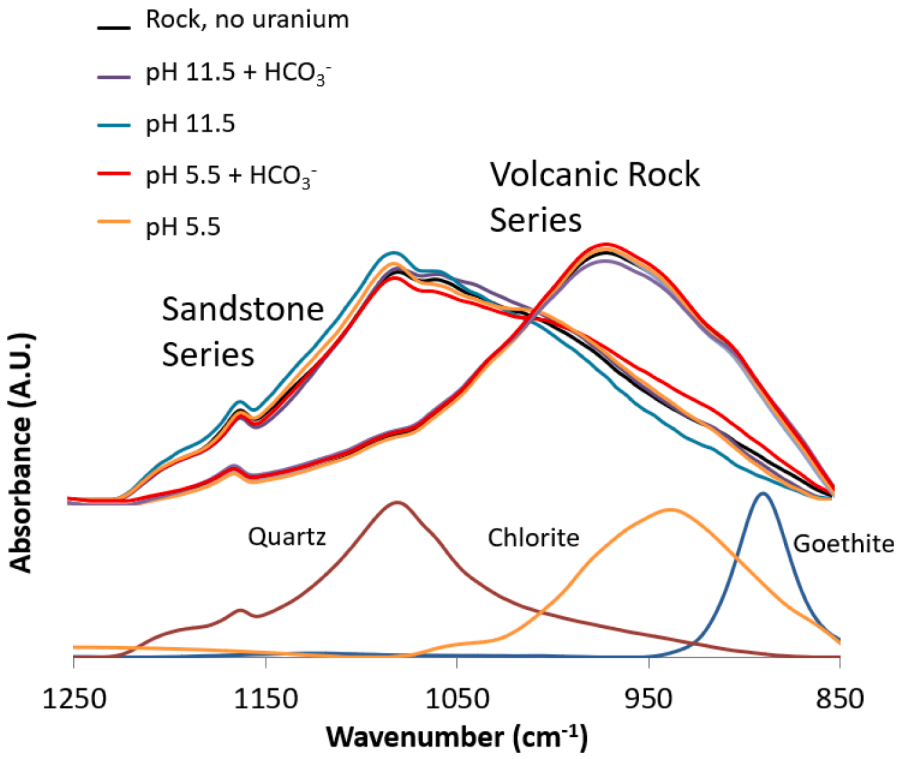

Fig. 1. FTIR spectra of U(VI) adsorbed on St. Bees Sandstone (SS) and Borrowdale Volcanic Group (BVG) in 0.1 M NaCl solution at pH 5.5 and pH 11.5 with or without of additions of 2 mM HCO_3^-.

and therefore it is likely that hematite is the iron oxide mineral that is coating the sandstone. This hematite-coating is in line with previous assumptions made in Kenney et al. [39], as they were unable to determine the mineralogy of the iron mineral in the St. Bees Sandstone with XRD due to the low relative concentration of the iron.

There is little change in the sandstone spectra after the 24-hour equilibration of U(VI) solutions at pH 5.5 and 11.5, with and without the addition of HCO_3^-, except for some variation in the shoulder at 912 cm^{-1}. This may relate to variations in the amount of iron oxide on the surface of the sandstone with respect to the quartz concentration. It is unlikely that this peak relates to the precipitation of a uranyl mineral in the pH 11.5 solution, since there is a decrease in the peak at 912 cm^{-1} at pH 11.5, where we would expect to see precipitation. However, there is an increase in the peak at 912 cm^{-1} in the experiment conducted at pH 5.5 with HCO_3^- added, in line with expected peaks due to the formation of surface complexes. If U was adsorbing to Fe-O, we would expect a shift to lower wavenumbers, which is not observed. The peak at 912 cm^{-1} only shows changes in magnitude; therefore, differences are primarily due to variations in the amount of Fe-O in the system, and thereby in the iron oxide coating thickness- potentially from dissolution. This is especially likely since Kenney et al. [39] observed small amounts of Fe in solution following experiments above pH 8. If there is precipitation of U on the surface of the sandstone, it is likely a minor phenomenon, because the concentration of U is below the detection limits of FTIR.

The infrared spectra of the volcanic rock exhibit the same peaks belonging to quartz (1195, 1161, and 1078 cm^{-1}). Furthermore, peaks at 1222, 935, and 900 cm^{-1} were observed. The peak at 1222 cm^{-1} is likely a contribution from the C—O bonds within calcite, the peak at 935 cm^{-1} from chlorite, which has a peak at 935 cm^{-1} in our standard, and the peak at 900 cm^{-1} is likely a contribution from the Fe—O—H bonds in the chlorite and mica, with a possibility of trace amounts of iron oxide minerals in the volcanic rock due to weathering. The spectral variations among the sandstone samples were small, whereas the volcanic rock samples did not show any changes during the experiments (as shown in Fig. 1). Like the sandstone, the concentration of U associated with the surface of the volcanic rock was too low to be detected. Therefore, analysis of the EXAFS data was used to interpret the surface coordination of uranium.

3.1.2. *Potentiometric titrations*

The results from the potentiometric titration experiments for sandstone and volcanic rock appear in Fig. S1A and S1B, respectively (Supplementary material). The data show three separate "forward" titrations of rock materials. The data are presented as the buffering capacity, which is defined as the concentration of acid [a] minus the concentration of base [b] normalised to the mass of rock (g) at each step of the titration, as a function of pH (Fig. S2; see Supplementary material). The buffering capacity of the rocks between pH 3–10 is $(1.64 \pm 0.22) \times 10^{-2}$ mol/g for the sandstone and $(1.13 \pm 0.34) \times 10^{-2}$ mol/g for the volcanic rock. This buffering capacity is like what has been measured for clay-rich soils [48]. A comparison between the forward and the reverse titrations is shown in Fig. S2. We observed no significant hysteresis in the sandstone or volcanic rock systems. With the volcanic rock, there was a very small difference between the forward and reverse titrations. However, the differences observed in the forward and reverse titration were generally smaller than the differences between the replicates, confirming this hysteresis to be insignificant. With insignificant hysteresis between the forward and reverse titrations, and the lack of changes in the FTIR spectra between pH 5.5 and 11.5 for either the sandstone or the volcanic rock over the course of the experiments, we can therefore assume that our washing procedure removed any loosely bound surface contamination and that there was no observed dissolution of the rocks over the course of our experiments.

3.1.3. *Surface complexation modelling*

The potentiometric titration data in our study were modelled using a NEM to determine the proton binding constants and site densities for the sandstone and volcanic rock (Fig. 2). The NEM approach was chosen as it accurately describes surface sites of complex multi-site systems (e.g. [18,49,2,38,12], and enables comparison with other studies using SCM.

The goodness of fit for each of the models was calculated using the residual V(Y) function, with V(Y) values between 0.1 and 20 indicating a good fit [64]. These values are determined for aqueous species in solution, and the range of acceptable error can be higher for multi-mineral suspensions [33]. Sandstone and volcanic rock were modelled so that the lowest V(Y) value could be achieved, using the minimum number of sites required to fit the model as to prevent over-fitting the data, which provided average V(Y) values of 23.09 ± 23.11 and 14.20 ± 6.11 for sandstone and volcanic rock, respectively. The sandstone was modelled with 2 surface sites and the volcanic rock with 3 surface sites. Attempts to model the data with less sites resulted in worsening V(Y) values (V(Y) > 40).

To model proton sorption onto the sandstone, two different sites are required, with pK_a values of 5.08 ± 0.12 and 8.81 ± 0.14, with site concentrations of (9.14 ± 4.83) × 10^{-6} and (4.00 ± 2.09) × 10^{-6} mol of sites/m^2, respectively (Table 2). To model proton sorption onto the volcanic rock, 3 sites are required, having pK_a values of 4.83 ± 0.07, 6.51 ± 0.16. and 8.89 ± 0.14, with site concentrations of (4.41 ± 0.46) × 10^{-6}, (3.15 ± 1.26) × 10^{-6} and (3.60 ± 0.46) × 10^{-6} mol of sites/m^2, respectively (Table 2).

3.2. Speciation of uranium

Speciation calculations of the aqueous solutions were previously conducted using Andra's SIT database in PHREEQC using the method outlined in Kenney et al. [39] (more details given in the Supplementary materials). We included the major element data collected in Kenney et al. [39] from sandstone and volcanic rock equilibrated in 0.1 M NaCl for 24 h, as a function of pH (Fig. S3). Therefore, in our equilibrated system the dominant species in solution at pH 5.5 were $UO_2CO_3^0$ and $(UO_2)_2(CO_3)(OH)_3^-$ when 2 mM HCO_3^- was added to solution, and UO_2^{2+} and $(UO_2)_3(OH)_5^+$ when it was not added. At pH 11.5 the dominant species in solution were $UO_2(OH)_3^-$ and $UO_2(OH)_4^{-2}$ when 2 mM HCO_3^- was not added to solution, and $UO_2(OH)_3^-$, $UO_2(OH)_4^{-2}$, and $UO_2(CO_3)_3^{4-}$ when HCO_3^- was added. Despite the differing major element concentrations in the sandstone and volcanic rock equilibrated solutions, similar species of U were present in solution over the pH range of this study (see [39] and Fig S3). Therefore, we expect that at low pH, differences will be dependent on uranyl carbonate/hydroxyl speciation, whereas at high pH, differences would be controlled by interaction with the mineral surfaces instead of from carbonate added to solution.

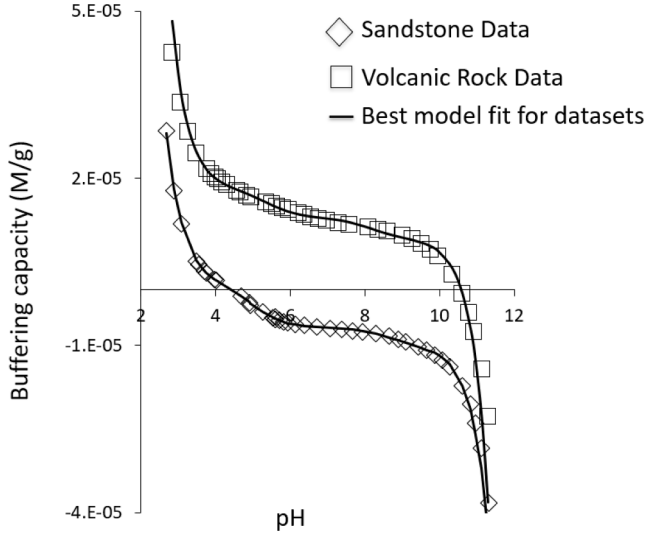

Fig. 2. Potentiometric titration data showing the data for sandstone (open diamonds) and volcanic rock (open squares) and the best model fits for each dataset (black line) in 0.1 M NaCl solutions. Data is plotted as the buffering capacity ([acid]-[base]) normalised to the mass of rock in suspension (g), as a function of pH.

Table 2
Acidity constants and site concentrations determined from modelling the potentiometric titrations for the sandstone and volcanic rock.

Rock	pK_a1	pK_a2	pK_a3	Site 1*	Site 2*	Site 3*	Total sites*
Sandstone	5.08 ± 0.12	8.81 ± 0.14	–	(9.14 ± 4.83) × 10^{-6}	(4.00 ± 2.09) × 10^{-6}	–	(1.31 ± 0.69) × 10^{-5}
Volcanic Rock	4.83 ± 0.07	6.51 ± 0.16	8.89 ± 0.14	(4.41 ± 0.46) × 10^{-6}	(3.15 ± 1.26) × 10^{-6}	(3.60 ± 0.46) × 10^{-6}	(1.12 ± 0.22) × 10^{-5}

*Concentration in moles of sites/m^2 of rock.

3.3. Uranium retention by sandstone and volcanic rock

The extent of U removal from solution by sandstone and volcanic rock, from a starting solution of 10 ppm U(VI) in 0.1 M NaCl, with and without the presence of carbonic acid, was described by Kenney et al. [39]. The pH values chosen for our experiments, 5.5 and 11.5, lie within the pH ranges of the two modes of removal of U from solution by both the sandstone and volcanic rock. The method details from the experiments are detailed in Table 1 and the percent of U removed from solution is illustrated in Fig. 3 along with the percentage of U removal from solution as observed by Kenney et al. [39]. Data from Kenney et al. [39] are reproduced with permission from the Royal Society of Chemistry. The extent of U removal from solution in this study is similar to what was removed in our previous work [39].

The raw and fitted κ^3-weighted U L_{III}-edge EXAFS data are shown in Fig. 4, with the fitting parameters presented in Table 3 for sandstone and volcanic rock, respectively. The signal to noise ratio decreases as pH is increased to pH 11.5, with the best spectra being fit up to 12 $Å^{-1}$. The low signal is likely related to the higher U loading since the U was likely precipitating on the rock surface. The sandstone and volcanic rock samples at pH 11.5 (with and without HCO_3^- added) show a broad double peak between 6 and 9.5 $Å^{-1}$, whereas the sandstone and volcanic rock samples at pH 5.5 (with and without HCO_3^- added) have a single peak between 6 and 9 $Å^{-1}$. This indicates that there are different U bonding environments between the high and low pH samples. The presence of two or more additional pair contributions that would interfere either constructively or destructively will produce similar spectra. The different combinations of these are generated by each of contribution of the local atomic environment around the U atoms. The exception to this trend may be the sandstone at pH 11.5 with added HCO_3^-, where there is significant noise and modelling may not capture the true bonding environment. This is discussed in detail in section 4.2.

4. Discussion

4.1. Characterisation of sandstone and volcanic rock surfaces

From the surface complexation modelling, the pK_a values for sandstone were 5.08 and 8.81 and for volcanic rock were 4.83 and 8.89, which are like what has been previously determined for the deprotonation of Fe-OH_2^+ to Fe-OH (4.3–6.1) and Fe-OH to Fe-O^- (8.1–9.8) in iron oxides and iron-coated sands [24,57,3,36]. For the volcanic rock, the pK_a value that was not seen in the sandstone system (6.51) may be related to the deprotonation of the $H_2CO_3^+$ surface species to HCO_3^0 for carbonates [65]. The pK_a value of 6.51 in the volcanic rock may be attributed to the silanol group (pK_a of 6.4–7.7; [41,54,9,44,21,34]) and thereby both silanol and carbonate groups may be active functional groups at the surface of the volcanic rock. The reason this site is not seen in the sandstone titrations is likely due to the surface coating of iron

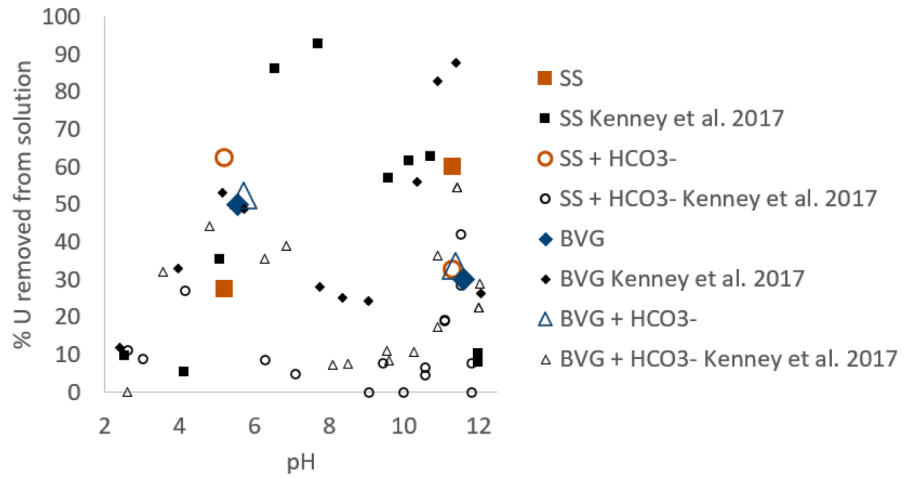

Fig. 3. U removal batch experiments, showing the removal of U by sandstone (orange) and volcanic rock (blue) both with (open shapes) and without (filled shapes) the addition of 2 mM HCO_3^- in 0.1 M NaCl solutions. Black shapes represent data reproduced from Kenney et al. [39] with permission from the Royal Society of Chemistry.

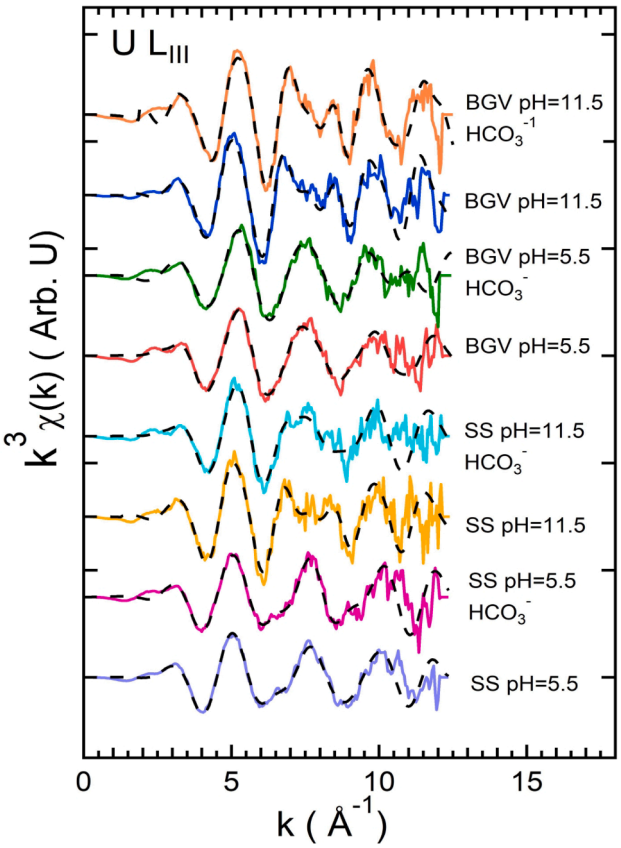

Fig. 4. Raw and fitted U L_{III}-edge κ^3-weighted EXAFS data for U(VI) removed from solution by the Borrowdale Volcanic Group (BVG) and St. Bees Sandstone (SS) in air equilibrated aqueous 0.1 M NaCl solution at pH 5.5 and pH 11.5 with or without of additions of 2 mM HCO_3^-.

oxide.

XRD analysis conducted in our previous study [39] was unable to detect an iron oxide coating on the sandstone due to it being present as a very thin coating on the quartz-rich sand. In this study, the FTIR spectroscopic analysis shows that Si-OH and Fe-OH groups in the volcanic rock had little variability throughout the experiments. In the sandstone system, however, we found that the layer of iron oxide on the surface (which we identified as hematite) varied in thickness across different samples. The surface complexation modelling mainly reflects the interactions of the outermost functional groups with the solution. In contrast, XRD and FTIR analyses provided information about the bulk properties of the sample, including its overall composition and structure.

4.2. Uranium speciation at the water–rock interface

The modelling parameters for the interaction of uranyl species with sandstone and volcanic rock are tabulated in Table 3. Errors in distance (±0.02 Å) and coordination numbers (±20%) are estimated from the deviation between fitting results from models of known structures and their values. For sandstone, the axial U-O distances were 1.78 Å for pH 5.5 and pH 5.5 with HCO_3^-. The pH 5.5 samples with and without HCO_3^- had equatorial U-O distances at 2.45 Å and at 2.49 Å, respectively, consistent with U(VI). The pH 5.5 sandstone sample with HCO_3^- had a U-Si distance of 3.25 Å, whereas the pH 5.5 sandstone sample without HCO_3^- had a U-Si distance of 3.33 Å. The pH 5.5 sandstone sample with HCO_3^- had a U-C bond distance of 3.05 Å. U was expected to be present in solution as a uranyl carbonate based on the speciation calculations in Fig. S3, itself based on the water chemistry provided in Kenney et al. [39]. In the sandstone pH 5.5 experiment without HCO_3^- added, the fitting indicates that U is adsorbed as a bidentate species to a single Si atom, most likely to quartz. In the case of the sandstone pH 5.5 experiment with HCO_3^- added, the fitting indicates that U is adsorbed to quartz as a bidentate carbonate species. Sylwester et al. [56] described similar U bonding environments where U was bound to silicate as a bidentate species to Si atoms. This is also like what was seen by Wang et al. [62]. A generalised conceptual model for our interpretation of these two adsorption complexes, as well as the rest of the U binding structures from this study, is given in Fig. 5.

For the sandstone experiments at pH 11.5, the axial and equatorial oxygen distances in the absence of HCO_3^- (1.81, and 2.41 Å, respectively) and with HCO_3^- (1.81, and 2.40 Å, respectively) were similar. For the pH 11.5 sample without bicarbonate, the Si coordination was split, with one Si coordinated at 3.24 Å and three Si coordinated at 4.11 Å. Additionally, there were three U-U distances at 4.19 Å. This is indicative of the formation of a U-Si mineral, likely soddyite with a U-Si distance of 3.14 Å [20] or an amorphous coffinite as was seen in lake sediments by Lefebvre et al. [43], having Si distances at 3.13 and 3.83 Å and a U-U distance at 3.83 Å. In addition to this U-Si precipitate, U exists as a sorbed bidentate species, like what was seen in the pH 5.5 sample without bicarbonate.

For the sample at pH 11.5 when bicarbonate was added, U may be present as a combination of a precipitated U-Na mineral and an

Table 3
EXAFS structural results for (UO_2^{2+}) complexes at surfaces of the sandstone (SS) and volcanic rock (BVG) using experimental conditions from Table 1. For Debye-Waller factor (σ^2 ($Å^2$)) results see Table S2.

Rock type		BVG	BVG	*BVG*	*BVG*	*SS*	*SS*	*SS*	*SS*
pH		pH = 5.5	pH = 5.5	*pH = 11.5*	*pH = 11.5*	*pH = 5.5*	*pH = 5.5*	*pH = 11.5*	*pH = 11.5*
HCO_3– added		N/A	2 mM HCO_3–	N/A	2 mM HCO_3–	N/A	2 mM HCO_3–	N/A	2 mM HCO_3–
U-O	*N*	2	2	2	2	2	2	2	2
	D (Å)	1.80 ± 0.01	1.78 ± 0.01	1.81 ± 0.02	1.82 ± 0.01	1.78 ± 0.01	1.78 ± 0.01	1.81 ± 0.01	1.81 ± 0.02
U-O	*N*	**5**	**5**	**5**	**5**	**5**	**5**	**5**	**5**
	D (Å)	2.38 ± 0.03	2.32 ± 0.02	2.40 ± 0.03	2.38 ± 0.01	2.45±	2.49 ± 0.01	2.41 ± 0.04	2.40 ± 0.01
U-Si	*N*			**1**	**1**	**1**	**0.5**	**1/3**	
	D (Å)			3.26 ± 0.03	3.26 ± 0.09	3.33 ± 0.07	3.25 ± 0.08	3.24 ± 0.03 / 4.11 ± 0.03	
U-C	*N*				**2**		**1**		**1**
	D (Å)				3.05 ± 0.2		3.05 ± 0.05		3.81 ± 0.10
U-Na	*N*			**3**					**3**
	D (Å)			3.77 ± 0.02					3.81±
U-U	*N*							**3**	**3**
	D (Å)							4.18 ± 0.08	3.88 ± 0.06

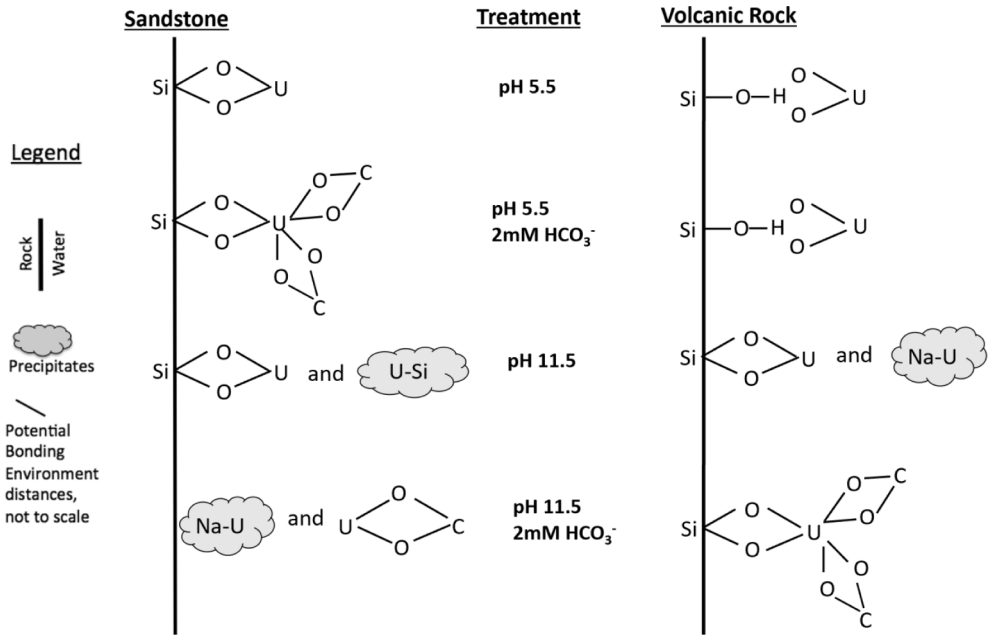

Fig. 5. Simplified conceptual model of uranyl sorption/precipitation onto sandstone (left) and volcanic rock (right), as a function of pH (pH 5.5 and 11.5) and bicarbonate content (none and 2 mM added).

unbonded uranyl carbonate species. The U-Na mineral may be Na-clarkeite with a U-Na distance of 3.78 Å [14], the same as was predicted to form in our previous study [39] and has been observed at the Hanford site [52]. Studies investigating U mineralogy at the Hanford site in Washington found that Na-boltwoodite was often found precipitated at the surface of and within fractures of feldspar minerals, where the dissolution of feldspar freed Si for the precipitation of the mineral [16,45]. Kenney et al. [39] noted Al in solution above pH 9; therefore, it is possible that the dissolution of the potassium feldspar in the sandstone ($KAlSi_3O_8$) led to the precipitation of Na-boltwoodite.

The modelling parameters for the interaction of uranyl species with volcanic rock are shown in Table 3. The axial U-O and equatorial U-O distances are 1.80 and 2.38 Å for pH 5.5 without HCO_3^- and 1.78 and 2.32 Å for pH 5.5 with HCO_3^-. The EXAFS data fits of these two samples could not be improved by the addition of another shell. Therefore, we conclude that both samples at pH 5.5 sorb U as an outer sphere complex, as can be seen in the conceptual model in Fig. 5.

For the high pH (11.5) volcanic rock experiments, the axial and equatorial oxygens were modelled with distances of 1.81 and 2.40 Å without HCO_3^-. The modelled U-Si distance was 3.26 Å and U-Na distance was 3.77 Å. The U-Si distance resembles that of bidentate U sorption to a single Si atom. The U-Na distances in this sample are like what was observed for the sandstone experiment at pH 11.5 with carbonate present. Therefore, we assume that either Na-clarkeite precipitates in the presence of the volcanic rock [28], or Na-boltwoodite, which may have precipitated via the dissolution of plagioclase.

The modelled axial and equatorial oxygen distances for the volcanic rock experiment at pH 11.5 with HCO_3^- were 1.82 and 2.38 Å, respectively. In addition, a U-Si distance of 3.26 Å and two U-C distances of 3.05 Å were calculated. Uranium binding is therefore attributed to the adsorption of U-carbonate species at the volcanic rock surface, like the binding environment in the sandstone experiment with HCO_3^- added at pH 5.5. This suggests adsorption of U-carbonate complexes to silicate minerals is important when interacting with rocks that have higher carbon content.

The conceptual models to depict these interpretations are shown in Fig. 5.

5. Conclusions

In this study we determined the mode of uranyl removal from solution by the St. Bees Sandstone and rocks from the Borrowdale Volcanic group, after first characterising the solid and aqueous components. Surface complexation modelling of potentiometric titration data revealed that the sandstone had two functional group types available for binding U based on the pH range of our modelling, both from the deprotonation of iron oxide surface coatings on the sand. Volcanic rock had three functional group types available for binding based on the pH range of our modelling, two from the amphoteric iron oxide functional group and one from silicates. The presence of these groups in the materials was confirmed via FTIR spectroscopy. EXAFS modelling determined that sorption of U onto silicate minerals at the rock surface was the primary means of U-removal from solution from both the sandstone and volcanic rock systems. At low pH, most U removal was due to adsorption. In the sandstone systems U was removed as uranyl or uranyl carbonates when bicarbonate was absent or present, respectively. In the volcanic rock system at low pH, the presence of bicarbonate did not affect U coordination, with uranyl species adsorbing as an outer sphere complex. In the high pH and no bicarbonate systems, uranyl both sorbed as a bidentate species to the silicate surface and precipitated. The mineral that precipitated in the bicarbonate-free high pH systems depended on the rock type present, with a U-Si mineral such as coffinite precipitating in the sandstone system and a mineral such as Na-boltwoodite in the volcanic rock system. The presence of bicarbonate changed the U-bonding environment in both the sandstone and volcanic rock systems at high pH. In the sandstone system, U existed as a U-carbonate species as well as precipitating as a mineral such as Na-clarkeite or Na-boltwoodite. In the volcanic rock system at high pH, the presence of carbonate halted the mineralization of U and instead it sorbed to Si as a uranyl carbonate species. These experiments strengthen the assumption in Kenney et al. [39] that uranyl sorption to the rocks was controlled by adsorption at low pH, but that U removal processes are more complex at high pH, with multiple U-removal processes controlling the chemistry. Furthermore, our results offer novel constraints on how heterogeneous rock material retains U, which reduces the number of assumptions required when modelling potential U transport at contaminated sites and potential long-term U storage facilities.

CRediT authorship contribution statement

Janice P.L. Kenney: Investigation, Writing – original draft, Writing – review & editing, Data curation, Project administration, Formal analysis, Methodology. **Juan Lezama-Pacheco:** Resources, Writing – review & editing, Data curation, Formal analysis, Software, Methodology. **Scott Fendorf:** Conceptualization, Resources, Funding acquisition, Software, Methodology. **Daniel S. Alessi:** Writing – review & editing, Investigation, Methodology. **Dominik J. Weiss:** Conceptualization, Funding acquisition, Supervision, Writing – review & editing, Data curation, Resources, Formal analysis, Methodology.

Declaration of Competing Interest

The authors declare that they have no known competing financial interests or personal relationships that could have appeared to influence the work reported in this paper.

Data availability

Data will be made available on request.

Acknowledgements

We acknowledge the Natural Environment Research Council, Radioactive Waste Management Limited, Environment Agency and Science and Technology Facilities Council for the funding received for this project through the Hydroframe consortium, part of the Radioactivity and the Environment (RATE) programme (NE/L000660/1). We thank SLS for access to the beamline and Stanford University for the Visiting Scholar support to DJW. We also thank the editor Prof. Max Lu and the anonymous reviewers, who helped improve this manuscript.

Appendix A. Supplementary data

Supplementary data to this article can be found online at https://doi.org/10.1016/j.jcis.2023.04.174.

References

[1] D.S. Alessi, J.B. Fein, Cadmium absorption onto mixtures of soil components: Testing the component additivity approach, Chem. Geol. 270 (1–2) (2010) 186–195.
[2] S.M. Alam, L. Swaren, K. von Gunten, M. Cossio, B. Bishop, L.J. Robbins, D. Hou, S. L. Flynn, Y. Sik Ok, K.O. Konhauser, D.S. Alessi, Application of surface complexation modeling to trace metals uptake by biochar-amended agricultural soils, Appl. Geochem. v88 (2018) 103–112.
[3] D.A. Ams, J.B. Fein, H. Dong, P.A. Maurice, Experimental Measurements of the Adsorption of Bacillus subtilis and Pseudomonas mendocina Onto Fe-Oxyhydroxide-Coated and Uncoated Quartz Grains, Geomicrobiol J. 21 (8) (2004) 511–519.
[4] Y. Arai, M. McBeath, J.R. Bargar, J. Joye, J.A. Davis, Uranyl adsorption and surface speciation at the imogolite–water interface: Self-consistent spectroscopic and surface complexation models, Geochim. Cosmochim. Acta v70 i10 (2006) 2492–2509.
[5] J.R. Bargar, K.H. Williams, K.M. Cambell, P.E. Long, J.E. Stubbs, E. Suvorova, J. S. Lezama-Pacheco, D.S. Alessi, M. Stylo, S.M. Webb, J.A. Davis, D.E. Giammar, L. Y. Blue, R. Bernier-Latmani, Uranium redox transition pathways in acetate-amended sediments, Proc. Natl. Acad. Sci. 110 (12) (2013) 4506–4511.
[6] J.R. Bargar, R. Reitmeyer, J.J. Lenhart, J.A. Davis, Characterization of U(VI)-carbonato ternary complexes on hematite: EXAFS and electrophoretic mobility measurements, Geochim. Cosmochim. Acta 64 (2000) 2737–2749.
[7] Y. Barthe, M. Elam, G. Sundqvist, Technological Fix or Divisible Object of Collective Concern? Histories of Conflict over the Geological Disposal of Nuclear Waste in Sweden and France, Sci. Cult. v29, i2 (2019) 196–218.
[8] Bond, D.L., Davis, J.A., Zachara, J.M., 2007, Chapter 14 Uranium(VI) Release from Contaminated Vadose Zone Sediments: Estimation of Potential Contributions from Dissolution and Desorption, Developments in Earth and Environmental Sciences, v7, p375-416.
[9] P. Bonnissel-Gissinger, M. Alnot, J.P. Lickes, J.J. Ehrhardt, P. Behra, Modeling the Adsorption of Mercury(II) on (Hydr)oxides II: a-FeOOH (Goethite) and Amorphous Silica, J. Colloid Interface Sci. 215 (1999) 313–322.
[10] D.M. Borrok, J.B. Fein, The impact of ionic strength on the adsorption of protons, Pb, Cd, and Sr onto the surfaces of Gram negative bacteria: testing non-electrostatic, diffuse, and triple-layer models, J Colloid Interface Sci 286 (2005) 110–126.
[11] P. Bots, K. Morris, R. Hibberd, G.T.W. Law, J.F.W. Mosselmans, A.P. Brown, J. Doutch, A.J. Smith, S. Shaw, Formation of stable uranium (VI) colloidal nanoparticles in conditions relevant to radioactive waste disposal, Langmuir 30 (2014) 14396–14405.
[12] J.C. Bullen, J.P.L. Kenney, S. Fearn, A. Kafizas, S. Skinner, D.J. Weiss, Improved accuracy in multicomponent surface complexation models using surface-sensitive analytical techniques: Adsorption of arsenic onto a TiO2/Fe2O3 multifunctional sorbent, J. Colloid Interface Sci. 580 (2020) 834–849.
[13] P.C. Burns, R.C. Ewing, F.C. Hawthorne, The crystal chemistry of hexavalent uranium: polyhedron geometries, bond-valence parameters, and polymerization of polyhedra, Can. Mineral. v35 (1997) 1551–1570.
[14] J.G. Catalano, G.E. Brown, Analysis of uranyl-bearing phases by EXAFS spectroscopy: Interferences, multiple scattering, accuracy of structural parameters, and spectral differences, Am. Mineral. 89 (2004) 1004–1021.
[15] J.G. Catalano, G.E. Brown, Uranyl adsorption onto montmorillonite: Evaluation of binding sites and carbonate complexation, Geochim. Cosmochim. Acta 69 (2005) 2995–3005.
[16] J.G. Catalano, S.M. Heald, J.M. Zachara, G.E.J. Brown, Spectroscopic and diffraction study of uranium speciation in contaminated vadose zone sediments from the Hanford site, Washington. Env. Sci. Tech. 38 (2004) 2822–2828.
[17] Cummings, R. and Raaz,D., 2011, LLW Repository Ltd Environmental Safety Case LLWR/ESC/R(11)10021.
[18] J.A. Davis, J.A. Coston, D.B. Kent, C.C. Fuller, Application of the surface complexation concept to complex mineral assemblages, Environ. Sci. Technol. 32 (1998) 2820–2828.
[19] De Windt, L., Spycher, N., 2019. Reactive Transport Modeling: A Key Performance Assessment Tool for the Geologic Disposal of Nuclear Waste, Elements, v15 99-102.
[20] F. Demartin, C.M. Gramaccioli, T. Pilati, The importance of accurate crystal structure determination of uranium minerals, II. Soddyite (UO2)2(SiO4).2H2O. Acta Crystallographica Section C. v48 (1992) 1–4.
[21] S. Dixit, P. Van Cappellen, Surface chemistry and reactivity of biogenic silica, Geochim. Cosmochim. Acta 66 (2002) 2559–2568.

[22] M.C. Duff, C. Amrhein, Uranium(VI) adsorption on goethite and soil in carbonate solutions, Soil Sci. Am. J. 60 (1996) 1393–1400.
[23] M.C. Duff, J.U. Coughlin, D.B. Hunter, Uranium co-precipitation with iron oxide minerals, Geochim. Cosmochim. Acta 66 (2002) 3533–3547.
[24] D.A. Dzombak, F.M.M. Morel, Surface complexation modeling: hydrous ferric oxide, Wiley-Interscience, New York, 1990.
[25] P.H. Eilers, Parametric time warping, Anal. Chem. 76 (2004) 404–411.
[26] J.B. Fein, C.J. Daughney, N. Yee, T.A. Davis, A chemical equilibrium model for metal adsorption onto bacterial surfaces, Geochim. Cosmochim. Act. v61 (1997) 3319–3328.
[27] J. Felten, H. Hall, J. Jaumot, R. Tauler, A. de Juan, A. Gorzsás, Vibrational spectroscopic image analysis of biological material using multivariate curve resolution-alternating least squares (MCR-ALS) Nat, Protoc. 10 (2) (2015) 217–240.
[28] R.J. Finch, R.C. Ewing, Am. Mineral. 82 (1997) 607–619.
[29] P.M. Fox, J.A. Davis, J.M. Zachara, The effect of calcium on aqueous uranium (VI) speciation and adsorption to ferrihydrite and quartz, Geochim. Cosmochim. Acta 70 (2006) 1379–1387.
[30] Francis, A. J., Cather,R. and Crossland, I. G. 1997, Nirex Science Report, S/97/014.
[31] D. Gorman-Lewis, J.B. Fein, P.C. Burns, J.E.S. Szymanowski, J. Converse, Solubility measurements of the uranyl oxide hydrate phases metaschoepite, compreignacite, Na–compreignacite, becquerelite, and clarkeite, J. Chem. Thermodynamics 40 (2008) 980–990.
[32] S. Ghaedi, K. Seifpanahi-Shabani, M. Sillanpää, Waste-to-Resource: New application of modified mine silicate waste to remove Pb2+ ion and methylene blue dye, adsorption properties, mechanism of action and recycling, Chemosphere 292 (2022), 133412.
[33] H.C.B. Hansen, T.P. Wetche, K. Raulund-Rasmussen, O.K. Borggaard, Stability constants for silicate adsorbed to ferrihydrite, Clay Miner. 29 (1994) 341–350.
[34] N. Hao, S.M.J. Moysey, B.A. Powell, D. Ntarlagiannis, Comparison of the surface ion density of silica gel evaluated via spectral induced polarization versus acid–base titration, J. Appl. Geophys. 135 (2016) 427–435.
[35] K.J. Johnson, J.E.S. Szymanowski, D. Borrok, T.Q. Huynh, J.B. Fein, Proton and metal adsorption onto bacterial consortia: stability constants for metal-bacterial surface complexes, Chem. Geol. 239 (2007) 13–26.
[36] N. Jordon, N. Marmier, C. Lomenech, E. Giffaut, J.-J. Ehrhardt, Competition between selenium (IV) and silicic acid on the hematite surface, Chemosphere v75 (2009) 129–134.
[37] M.J. Kang, B.E. Han, P.S. Hahn, Precipitation and adsorption of uranium (VI) under various aqueous conditions, Environ. Eng. Res. v7, i3 (2002) p149–p157.
[38] J.P.L. Kenney, T. Ellis, F.S. Nicol, A.E. Porter, D.J. Weiss, The effect of bacterial growth phase and culture concentration on U(VI) removal from aqueous solution, Chem. Geol. 482 (2018) 61–71.
[39] J.P.L. Kenney, M.E. Kirby, J. Cuadros, D.J. Weiss, A conceptual model to predict uranium removal from aqueous solutions in water-rock systems associated with low- and intermediate-level radioactive waste disposal, RSC Adv. 7 (2017) 7876–7884.
[40] M.E. Kirby, J.S. Watson, J. Najorka, J.P.L. Kenney, S. Krevor, D.J. Weiss, Experimental study of pH effect on uranium (UVI) particle formation and transport through quartz sand in alkaline 0.1 M sodium chloride solutions, Colloids Surf A Physicochem Eng Asp 592 (2020), 124375.
[41] M. Kosmulski, Adsorption of cadmium on alumina and silica: analysis of the values of stability constants of surface complexes calculated for different parameters of triple layer model, Colloids Surf A Physicochem Eng Asp 117 (1996) 201–214.
[42] M. Laabd, Y. Brahmi, B. El Ibrahimi, A. Hsini, E. Toufik, Y. Abdellaoui, H. Abou Oualid, M. El Ouardi, A. Albourine, A novel mesoporous Hydroxyapatite@ Montmorillonite hybrid composite for high-performance removal of emerging Ciprofloxacin antibiotic from water: Integrated experimental and Monte Carlo computational assessment, J. Mol. Liq. 116705 (2021).
[43] P. Lefebvre, A. Gourgiotis, A. Mangeret, P. Sabatier, P. Le Pape, O. Diez, P. Louvat, N. Menguy, P. Merrot, C. Baya, M. Zebracki, P. Blanchart, E. Malet, D. Jézéquel, J. L. Reyss, J.R. Bargar, J. Gaillardet, C. Cazala, G. Morin, Diagenetic formation of uranium-silica polymers in lake sediments over 3,300 years, PNAS v118 (2021) (4).
[44] N. Marmier, A. Delisée, F. Fromage, Surface Complexation Modeling of Yb(III) and Cs(I) Sorption on Silica, J. Colloid Interface Sci. 212 (1999) 228–233.
[45] J.P. McKinley, J.M. Zachara, C. Liu, S.C. Heald, B.I. Prenitzer, B.W. Kempshall, Microscale controls on the fate of contaminant uranium in the vadose zone, Hanford Site, Washington, Geochim. Cosmochim. Acta 70 (2006) 1873–1887.
[46] P. Michard, E. Guibal, T. Vincent, P. Le Cloirec, Sorption and desorption of uranyl ions by silica gel: pH, particle size and porosity effects, Microporous Mater. 5 (1996) 309–324.
[47] S. Nair, B.J. Merkel, Impact of Alkaline Earth Metals on Aqueous Speciation of Uranium(VI) and Sorption on Quartz, Aquat Geochem 17 (2011) p209–p219.
[48] P.N. Nelson, N. Su, Soil pH buffering capacity: a descriptive function and its application to some acidic tropical soils, Soil Res. v48 (2009) 201–207.
[49] F. Pagnanelli, L. Bornoroni, E. Moscardini, L. Toro, Non-electrostatic surface complexation models for protons and lead (II) sorption onto single minerals and their mixture, Chemosphere 63 (2006) 1063–1073.
[50] Petrangeli, G., 2006. Nuclear Safety, Chapter 23 - Radioactive waste, Butterworth-Heinemann, Pages 221-223, ISBN 9780750667234.
[51] J.D. Prikryl, A. Jain, D.R. Turner, R.T. Pablan, Uranium(VI) sorption behaviour on silicate mineral mixtures, J. Contam. Hydrol. 47 (2001) 241–253.
[52] J.G. Reynolds, G.A. Cooke, J.S. Page, R.W. Warrant, Uranium-bearing phases in Hanford nuclear waste, J. Radioanal. Nucl. Chem. 316 (2018) 289–299.
[53] H.D. Ruan, R.L. Frost, J.T. Kloprogge, L. Duong, Infrared spectroscopy of goethite dehydroxylation: III. FT-IR microscopy of in situ study of the thermal transformation of goethite to hematite, Spectrochim. Acta A Mol. Biomol. Spectrosc. 58 (2002) 967–981.
[54] N. Sahai, D.A. Sverjensky, Evaluation of internally consistent parameters for the triple-layer model by the systematic analysis of oxide surface titration data, Geochim. Cosmochim. Acta 61 (1997) 2801–2826.
[55] Savitzky, A., GolayM.J.E., 1964. Smoothing and differentiation of data by simplified least squares procedures Anal. Chem., 36, 1627-1639.
[56] E.R. Sylwester, E.A. Hudson, P.G. Allen, The structure of uranium (VI) sorption complexes on silica, alumina, and montmorillonite, Geochim. Cosmochim. Acta 64 (2000) 2431–2438.
[57] C.J. Tadanier, M.J. Eick, Formulating the Charge-distribution Multisite Surface Complexation Model Using FITEQL, Soil Sci. Soc. Am. J. v66 (2002) 1505–1517.
[58] E. Theodosoglou, A. Koroneos, T. Soldatos, T. Zorba, K.M. Paraskevopoulous, Comparative Fourier transform infrared and X-ray powder diffraction analysis of naturally occurred K-feldspars. Bulletin of the Geological Society of Greece, 2010.
[59] K.V. Ticknor, Uranium sorption on geological materials, Radiochim. Acta 64 (1994) 229–236.
[60] C. Tournassat, R.M. Tinnacher, S. Grangeon, J.A. Davis, Modeling uranium(VI) adsorption onto montmorillonite under varying carbonate concentrations: A surface complexation model accounting for the spillover effect on surface potential, Geochim. Cosmochim. Acta 220 (2018) 291–308.
[61] T.D. Waite, J.A. Davis, T.E. Payne, G.A. Waychunas, N. Xu, Uranium(VI) adsorption to ferrihydrite: Application of a surface complexation model, Geochim. Cosmochim. Acta 58 (1994) 5465–5478.
[62] Z. Wang, J.M. Zachara, J.-F. Boily, Y. Xia, T.C. Resch, D.A. Moore, C. Liu, Determining individual mineral contributions to U(VI) adsorption in a contaminated aquifer sediment: A fluorescence spectroscopy study, Geochim. Cosmochim. Acta 75 (10) (2011) 2965–2979.
[63] S.M. Webb, Physica Scripta SIXpack: a graphical user interface for XAS analysis using IFEFFIT, Phys. Scr. v2005, T115 (2005) 1011–1014.
[64] J.C. Westall, FITEQL: A computer program for determination of chemical equilibrium constants from experimental data, Oregon State University, Chemistry Department, 1982.
[65] M. Wolthers, L. Charlet, P. Van Cappellen, The surface chemistry of divalent metal carbonate minerals; a critical assessment of surface charge and potential data using the charge distribution multi-site ion complexation model, Am. J. Sci. 308 (2008) 905–941.
[66] N. Yee, J.B. Fein, Does metal adsorption onto bacterial surfaces inhibit or enhance aqueous metal transport? Column and batch reactor experiments on Cd–Bacillus subtilis–quartz systems, Chem. Geol. 2002 (185) (2002) 303–319.